

# Transport regimes in surface disordered graphene sheets

E. Louis,<sup>1</sup> J. A. Vergés,<sup>2</sup> F. Guinea,<sup>2</sup> and G. Chiappe<sup>1,3</sup>

<sup>1</sup>*Departamento de Física Aplicada, Unidad Asociada del Consejo Superior de Investigaciones Científicas and Instituto Universitario de Materiales, Universidad de Alicante, San Vicente del Raspeig, Alicante 03690, Spain.*

<sup>2</sup>*Departamento de Teoría de la Materia Condensada, Instituto de Ciencias de Materiales de Madrid (CSIC), Cantoblanco, Madrid 28049, Spain*

<sup>3</sup>*Departamento de Física J.J. Giambiagi, Facultad de Ciencias Exactas, Universidad de Buenos Aires, Ciudad Universitaria, 1428 Buenos Aires, Argentina.*

(Dated: September 13, 2018)

We investigate the size scaling of the conductance of surface disordered graphene sheets of width  $W$  and length  $L$ . Metallic leads are attached to the sample ends across its width. At the Dirac point,  $E = 0$ , the conductance scales with the system size as follows: i) For constant  $W/L$ , it remains constant as size is increased, at a value which depends almost linearly on that ratio; this scaling allows the definition of a conductivity value that results similar to the experimental one. ii) For fixed width, the conductance decreases exponentially with length  $L$ , both for ordered and disordered samples. Disorder reduces the exponential decay, leading to a higher conductance. iii) For constant length, conductance increases linearly with width  $W$ , a result that is exclusively due to the tails of the states of the metallic wide contact. iv) The average conductance does not show an appreciable dependence on magnetic field until fields such that the flux per unit cell approaches the quantum unit. Away from  $E = 0$ , the conductance shows the behavior expected in two-dimensional systems with surface disorder, i.e., ballistic transport.

PACS numbers: 73.63.Fg, 71.15.Mb

*Introduction.* The electronic transport in atomically thin graphene samples is a subject of great current interest [1, 2, 3, 4, 5, 6, 7]. The scaling with the sample dimensions [4] suggest a diffusive behavior, with a universal conductivity at the lowest carrier concentrations [4, 6]. The limit of low concentrations is difficult to analyze theoretically, as the Fermi wavelength becomes comparable to the separation between scatterers, and even to the sample size. An analysis based on the Born approximation [8] leads to a universal conductivity at low temperatures, although its value is somewhat smaller than the one observed experimentally. The approximations involved in this approach, however, are expected to fail at the lowest concentrations. Field theoretical arguments [9, 10, 11] suggest the existence of a localized regime in the limit of zero temperature and zero carrier concentration. At zero doping, clean graphene systems show an unusual scaling of the conductance on sample size, consistent with diffusive behavior [12]. This pseudo-diffusive behavior has also been found in SNS junctions [13] and graphene bilayers [14].

In this work, we numerically study the electronic transport in surface disordered graphene sheets both at finite dopings and in the limit of zero carrier concentration. As bulk disorder in graphene sheets seems to be rather low, we focus on the effects of rough edges, with disorder concentrated at the surface of the system. Our results show that the pseudo-diffusive regime identified in [12] persists in the presence of disorder, namely, near the band center the conductance is proportional to the sheet width and almost inversely proportional to its length. Although our

results fit apparently the requirements of diffusive scaling in 2D, a closer look reveals important differences. Certainly, when plotting the conductance of samples of fixed width as a function of the sample length, an exponential decrease is obtained, that is, the standard result for a quasi 1D system with any kind of disorder. The remarkable thing in graphene is that this exponential decrease survives in ordered samples. Actually, the presence of disorder slows down the exponential decay. These results can be rationalized in terms of transmission mediated by evanescent waves generated at the metallic leads. On the other hand, the conductance for fixed length is proportional to the sample width at all energies, a behavior that does not distinguish between diffusive and ballistic regimes. Finally, for sufficiently high carrier concentrations, the conductance shows the ballistic behavior expected in 2D systems with surface disorder, namely, increase with the system size for constant  $W/L$ , linear increase with  $W$  for constant  $L$ , and exponential decrease with  $L$  for constant  $W$ .

*Methods: graphene samples and conductance calculations.* We describe the valence and conduction bands of graphene by a tight binding hamiltonian with nearest neighbor hoppings only:

$$\mathcal{H} = t \sum_{i,j} c_i^\dagger c_j + h.c. \quad (1)$$

where sites  $i$  and  $j$  denote the nearest neighbor nodes in the honeycomb lattice. The low energy electronic spectrum,  $|\epsilon_{\mathbf{k}}| \ll t$ , can be approximated by the Dirac equa-

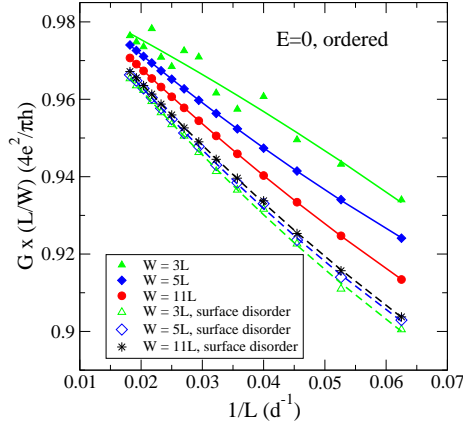


FIG. 1: (Color online) Scaling of the conductance of stripes of different widths,  $W$ , as function of length,  $L$ .

tion:

$$\epsilon_{\mathbf{k}} \approx \pm v_F |\tilde{\mathbf{k}}| \quad (2)$$

where  $v_F = (3td)/2$ , and  $d$  is the distance between sites in the honeycomb lattice.

Samples with surface disorder were produced by randomly removing sites at the sheet edges. The leads were simulated by a purely imaginary selfenergy independent of energy, that was attached across the sample width. In the interpretation of the numerical results for surface disordered sheets, perfect samples without and with Anderson disorder at its edges [15, 16] were also investigated. The latter was introduced by randomly sorting the orbital energies at the surface sites within the range  $[-\Delta, \Delta]$ .

The conductance was calculated by means of an efficient implementation of Kubo's formalism [17]. For a current propagating in the  $x$ -direction, the static electrical conductivity is given by:

$$\mathcal{G} = -2 \left( \frac{e^2}{h} \right) \text{Tr} \left[ (\hbar \hat{v}_x) \text{Im} \hat{G}(E) (\hbar \hat{v}_x) \text{Im} \hat{G}(E) \right], \quad (3)$$

where the velocity (current) operator  $\hat{v}_x$  is related to the position operator  $\hat{x}$  through the equation of motion  $\hbar \hat{v}_x = [\hat{H}, \hat{x}]$ ,  $\hat{H}$  being the Hamiltonian.  $\hat{G}(E)$  is the Green function of the system with the leads already incorporated. All results include the spin degeneracy.

**Results.** Fig.[1] shows typical results for stripes without and with disorder. At  $E = 0$ , the scaling of the conductance in clean samples as  $G = 4e^2/(\hbar\pi) \times W/L$  [12] is already obtained with high accuracy in not too wide samples. At higher energies,  $E = 0.5$ , the conductance becomes ballistic. This pseudodiffusive regime, was already analyzed in clean systems in [12]. In a clean square system, the incoming channels can be characterized by the transverse momentum,  $k_y$ . The electronic spectrum of a graphene stripe at finite transverse momentum shows a

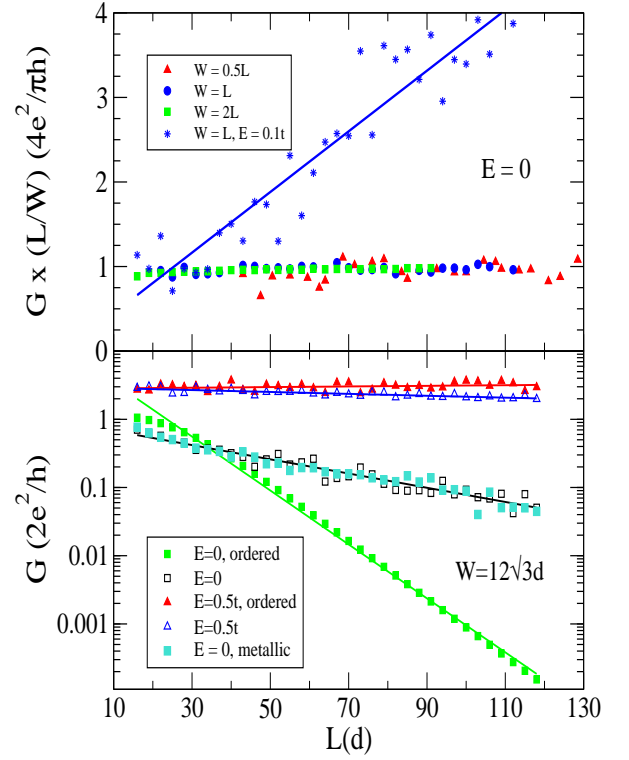


FIG. 2: (Color online) Top panel: Scaling with length  $L$  of the conductance in samples with width over length ratios and surface disorder. Bottom panel. Scaling with length of stripes of fixed width. The points labelled metallic correspond to a stripe with a subband crossing at  $E = 0$ . All other samples have finite size gaps near  $E = 0$ .

gap for  $-v_F |k_y| \leq \epsilon \leq v_F |k_y|$ . Hence, states with transverse momentum  $k_y$  decay away from the boundaries as  $e^{-|k_y|x}$ , and lead to a transmission  $T_{k_y} \propto e^{-2|k_y|L}$ , where  $L$  is the length of the system. The number of channels scale as the width of the system,  $W$ . In sufficiently large systems, the sum over channels can be replaced by an integral over  $k_y$  leading to a conductance  $G$  which scales as  $G \propto WL^{-1}$ . Away from  $E = 0$  the conductance increases linearly with the system size. This is the expected ballistic behavior of a quantum billiard with either surface disorder or with an amount of defects proportional to  $L$  (a defect concentration decreasing as  $1/L$ ) [15, 18].

The scaling of the conductance with stripe length in systems with surface disorder and different  $W/L$  ratios is shown in the upper panel of Fig.[2]. The conductance at  $E = 0.1$  deviates very slightly from ballistic behavior. Disordered samples show a length independent conductivity close to that estimated analytically in the clean limit [12], and this regime is attained even for widths smaller than the length. The conductance scales exponentially with  $L$ . In a clean systems, this behavior arises from the existence of minigaps separating subbands with well defined periodicity in the transverse direction. The corresponding decay length shorter in clean samples

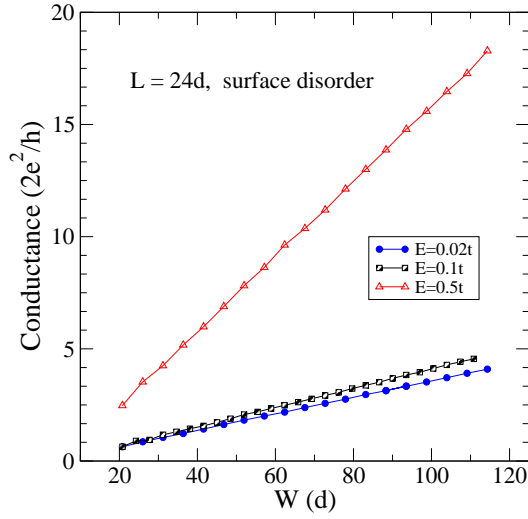


FIG. 3: (Color online) Conductance (in units of the conductance quantum) through surface disordered graphene samples of size  $W \times 24d$  versus the sample width  $W$  (in units of the C-C distance  $a$ ). Results for three energies are shown.

than in disordered samples, leading to an enhancement of the conductance in semiconducting disordered samples at  $E = 0$ .

The enhancement of the conductance in the localized regime in disordered samples is probably related to the formation of resonances at  $E = 0$  near defects. The existence of these resonances has been well established at edges[19, 20], cracks[21], and vacancies[22]. After the first version of this paper was posted, related resonances were discussed in the continuum limit[23]. Note that, in addition to  $E = 0$  resonances induced by disorder, long wavelength modulations of the chemical potential will move one of the edges of the gap at fixed parallel momentum towards  $E = 0$ , reducing the decay length and enhancing the conductance.

The scaling of the conductance with the width of a sheet of constant length is shown in Fig. 3. The numerical results clearly indicate that the conductance increases linearly with the sample width with a slope that depends on the concentration of carriers (or the energy). This result is characteristic of both ballistic and diffusive behaviors in 2D, and cannot therefore be used to discriminate the transport regime in this case. A remarkable feature of the results shown in Fig. 3 is its very low dispersion. This could be understood by noting that the increase in conductance is exclusively due to an increasing number of metallic tails through the bulk of the graphene sheet, and therefore weakly sensitive to surface disorder.

We show in Fig. 4 the dependence of the conductance on magnetic field for different disorder realizations [24]. The area of the sample,  $40d \times 40d$ , and 62 unit cells, is such that one flux unit through it is equivalent to approximately 660 Teslas. Hence, the magnetoresistance

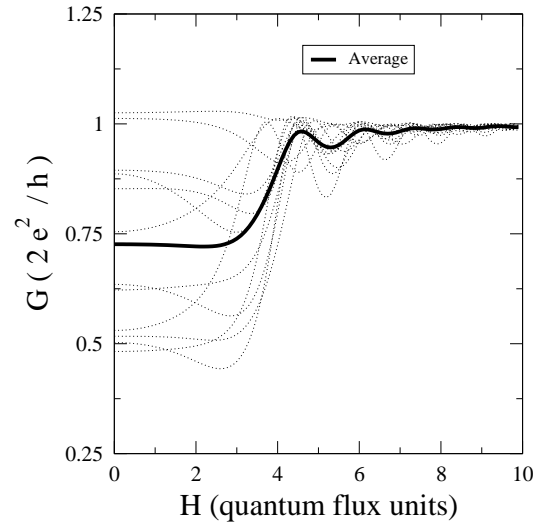


FIG. 4: (Color online) Conductance (in units of the conductance quantum) as function of the total magnetic flux through the graphene lattice in  $40d \times 40d$  clusters and  $E = 0.02$ , with disorder at the edges. A magnetic field of 1 Tesla corresponds, approximately, to 0.04 flux units through the cluster.

for fields attainable in the laboratory is negligible. This result is consistent with semianalytical calculations using a continuum model in the clean limit[25]. The magnetoresistance shows oscillations when the flux per unit cell is of order 0.05. At very high fields, the conductance becomes of order of one quantum unit, and it shows no dependence on disorder realization. Note that, in the regime studied here, the quasiclassical arguments used when discussing either weak localization or weak antilocalization effects in graphene cannot be used[26, 27, 28].

The study of the conductance distribution for samples of an approximate square shape at an energy  $E = 0.001t$  very close to the Dirac point further explains the role played by the metallic tails in the conductance behavior. Fig. 5 shows that conductance is larger than  $\approx 0.37(2e^2/h)$  for this geometry (the tails contribution that is minimally affected by surface disorder) and fluctuates below 1 as it does in a standard quantum billiard in the case of point contacts. The existence of an abrupt upper cutoff resembles the case studied in[29]. Nevertheless, a significant difference is clear; while the upper conductance limit is due to the incidence of only one channel in the billiard case, it is due to the intrinsic small number of channels (0 or 1) of graphene near the band-center.

*Concluding Remarks.* The numerical calculations of the conductance through surface disordered graphene sheets presented in this work reproduce the quasi-diffusive behavior found by other authors in ordered graphene at the Dirac point[12, 13, 14, 30]. Specifically, the conductance remains constant when the size of the system is increased, as opposed to the linear increase with the system size found at any other energy. However, we found this be-

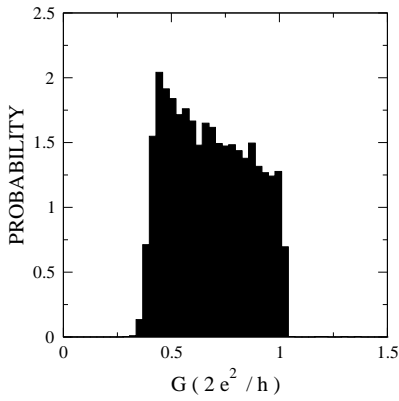


FIG. 5: Conductance distribution obtained at  $E = 0.001t$  for a set of 10,000 graphene randomly generated samples of size  $24d \times 24d$ . Surface disorder is restricted to a  $4d$  fringe around the sample surface. Good metallic contacts are attached at opposite sides of the sample.

havior only when the size of the system is increased in such a way that the width to length ratio is kept constant. A value of  $\approx 0.75(2e^2/h)$  is obtained for this pseudconductivity, not that far from the experimental one.

The conductance of the stripes calculated here changes qualitatively as the aspect ratio of the sample is varied. In stripes where the length is much larger than the width, the pseudodiffusive behavior described above is replaced by an exponential decay with length, a sign of localization. In this regime, disorder leads to longer decay lengths, probably due to the formation of resonances at the Dirac point,  $E = 0$ .

Finally, we have also shown that a magnetic field with a magnetic length much larger than the lattice spacing does not change appreciably the conductance near the Dirac point.

**Acknowledgments** Financial support by the Spanish MCYT (grants FIS200402356, MAT2005-07369-C03 and NAN2004-09183-C10-08), the Universidad de Alicante, the Generalitat Valenciana (grant GRUPOS03/092 and grant GV05/152), the Universidad de Buenos Aires (grant UBACYT x115) and the Argentinian CONICET is gratefully acknowledged. GC is thankful to the Spanish "Ministerio de Educación y Ciencia" for a Ramón y Cajal grant. F. G. acknowledges funding from MEC (Spain) through grant FIS2005-05478-C02-01 and the European Union Contract 12881 (NEST), and the Comunidad de Madrid, through the program CITECNOMIK, CM2006-S-0505-ESP-0337.

[1] K. S. Novoselov, A. K. Geim, S. V. Morozov, D. Jiang, Y. Zhang, S. V. Dubonos, I. V. Grigorieva, and A. A.

Firsov, *Science* **306**, 666 (2004).  
[2] C. Berger, Z. M. Song, T. B. Li, X. B. Li, A. Y. Ogbazghi, R. Feng, Z. T. Dai, A. N. Marchenkov, E. H. Conrad, P. N. First, et al., *J. Phys. Chem. B* **108**, 19912 (2004).  
[3] J. S. Bunch, Y. Yaish, M. Brink, K. Bolotin, and P. L. McEuen, *Nano Lett.* **5**, 2887 (2005).  
[4] K. S. Novoselov, A. K. Geim, S. V. Morozov, D. Jiang, M. I. Katsnelson, I. V. Grigorieva, S. V. Dubonos, and A. A. Firsov, *Nature* **438**, 197 (2005).  
[5] K. S. Novoselov, D. Jiang, F. Schedin, T. J. Booth, V. V. Khotkevich, S. V. Morozov, and A. K. Geim, *Proc. Nat. Acad. Sci.* **102**, 10451 (2005).  
[6] Y. Zhang, Y.-W. Tan, H. L. Stormer, and P. Kim, *Nature* **438**, 201 (2005).  
[7] S. V. Morozov, K. S. Novoselov, F. Schedin, D. Jiang, A. A. Firsov, and A. K. Geim, *Phys. Rev. B* **72**, 201401(R) (2005).  
[8] N. M. R. Peres, F. Guinea, and A. H. Castro Neto, *Phys. Rev. B* **73**, 125411 (2006).  
[9] I. L. Aleiner and K. B. Efetov (2006), cond-mat/0607200.  
[10] A. Altland (2006), cond-mat/0607247.  
[11] P. M. Ostrovsky, I. V. Gornyi, and A. D. Mirlin (2006), cond-mat/0609617.  
[12] J. Tworzydło, B. Trauzettel, M. Titov, A. Rycerz, and C. W. J. Beenakker, *Phys. Rev. Lett.* **96**, 246802 (2006).  
[13] M. Titov and C. W. J. Beenakker, *Phys. Rev. B* **74**, 041401(R) (2006).  
[14] I. Snymán and C. W. J. Beenakker (2006), cond-mat/0609243.  
[15] E. Cuevas, E. Louis, and J. A. Vergés, *Phys. Rev. Lett.* **77**, 1970 (1996).  
[16] E. Louis, E. Cuevas, J. A. Vergés, and M. Ortuno, *Phys. Rev. B* **56**, 2120 (1997).  
[17] J. A. Vergés, *Comp. Phys. Commun.* **118**, 71 (1999).  
[18] J. A. Vergés and E. Louis, *Phys. Rev. E* **59**, R3803 (1999).  
[19] K. Wakayabashi and M. Sigrist, *Phys. Rev. Lett.* **84**, 3390 (2000).  
[20] K. Wakayabashi, *Phys. Rev. B* **64**, 125428 (2001).  
[21] M. A. H. Vozmediano, M. P. López-Sancho, T. Stauber, and F. Guinea, *Phys. Rev. B* **72**, 155121 (2005).  
[22] V. M. Pereira, F. Guinea, J. M. B. L. dos Santos, N. M. R. Peres, and A. H. C. Neto, *Phys. Rev. Lett.* **96**, 036801 (2006).  
[23] M. Titov (2006), cond-mat/0611029.  
[24] E. Louis and J. A. Vergés, *Phys. Rev. B* **63**, 115310 (2001).  
[25] E. Prada, P. San-José, B. Wunsch, and F. Guinea (2006), cond-mat/0611189.  
[26] S. V. Morozov, K. Novoselov, M. Katsnelson, F. Schedin, D. Jiang, and A. K. Geim, *Phys. Rev. Lett.* **97**, 016801 (2006).  
[27] A. F. Morpurgo and F. Guinea, *Phys. Rev. Lett.* **97**, 196804 (2006).  
[28] E. McCann, K. Kechedzhi, V. I. Fal'ko, H. Suzuura, T. Ando, and B. L. Altshuler, *Phys. Rev. Lett.* **97**, 146805 (2006).  
[29] K. A. Muttalib, P. Wölffe, A. García-Martín, and V. A. Gopar, *Europhys. Lett.* **61**, 95 (2003).  
[30] C. W. J. Beenakker, *Phys. Rev. Lett.* **97**, 067007 (2006).